Real Options with Regulatory Policy Uncertainty

Christian Maxwell and Matt Davison

Abstract Energy Finance as a field is particularly bedeviled by regulatory uncertainty. This is notably the case for the real option analysis of long-lived energy infrastructure. How can one decide optimal build times on a 50 year project horizon when regulations regarding pricing and costs change on a much shorter time scale? In this paper we present a quantitative framework for modelling and interpreting regulatory changes for energy real options as a Poisson jump process, in a context where other relevant prices follow diffusion processes. We illustrate this conceptual framework with a case study involving the US corn ethanol market for which subsidy levels have experienced frequent changes. Subsidy levels have an easily quantified impact on operations and profitability, making this a nice arena to introduce ideas which might later be extended to less easily quantified regulatory changes. Numerical techniques are presented to solve the resulting partial integro differential variational inequalities. These solution techniques are deployed to solve instructive numerical examples, and conclusions for public policy are drawn.

1 Introduction

All large energy and natural resource projects are subject to government policy or regulation of some kind. These regulations are intended to achieve public policy goals and their effects should be taken into account by firms planning to enter into energy or resource investments. Energy and resource projects often have long project horizons and operating life spans on the order of decades. Consider the example of a firm deciding to enter into a 50 year energy production investment. Policy in terms of taxation, environmental regulations and other laws may materially affect project cash flows. These policies have been known to change. Some policy

C. Maxwell
Department of Applied Mathematics, University of Western Ontario, London, ON, Canada
e-mail: cmaxwel5@uwo.ca

M. Davison (✉)
Department of Statistical and Actuarial Sciences, University of Western Ontario, London, ON, Canada
e-mail: mdavison@uwo.ca

R. Aïd et al. (eds.), *Commodities, Energy and Environmental Finance*,
Fields Institute Communications 74, DOI 10.1007/978-1-4939-2733-3_9

amendments are well broadcast and announced while others are not. Although policy changes may appear "predictable" in the short term, forecasting onto a 50 year project horizon renders the policy changes apparently random, and hence requiring models of *policy uncertainty*.

Policy Uncertainty is characterized by changes in taxation, legal and other regulatory policies that affect a business' operations and profitability. The uncertainty derives from the inability to predict policy in the long term; uncertainty about forthcoming policy or announcements of policy changes; or sudden and abrupt changes in policy. Some anecdotal examples of policy uncertainty in energy and resource markets from recent North American news headlines follow:

Ontario Looks Set to Cut Green Energy Subsidies Solar rates expected to be cut substantially. Industry has 6 weeks to provide input. [31]

Ontario Drops Plan for TransCanada Power Plant Ontario cancels planned Trans Canada power plant with province to discuss compensation with TransCanada. Costs may exceed $1 billion CAD and affect off peak pricing. [24, 30]

Ivanhoe 'Surprised' by New Mongolian Windfall Tax Mongolia sets surprise windfall tax on (among possibly others) Ivanhoe's Oyu Tolgoi mine of 68 % when gold hits $500 per ounce. [7]

This does not by any means represent an exhaustive list. Attempts have been made to quantify and measure policy uncertainty (e.g. [3]). In [3] and [17] the authors also note that policy uncertainty can make firms hesitate or delay to enter into long term projects as they wait for more policy certainty before making decisions. This has caught the eye of Canadian and American macroeconomic policy makers noting both that firms appear to accumulate cash and hesitate to make business decisions amidst regulatory uncertainty [16, 35].

In this paper we present a quantitative framework for modelling and interpreting regulatory changes for energy real options as a jump diffusion process, in a context where other relevant prices follow pure diffusion processes. Policy uncertainty is by its nature very difficult to hedge and leads to market incompleteness even if the remaining underlying prices could otherwise be traded.

This real option method of modelling resource project management decisions was introduced by [6] in a seminal paper that considered the problem of optimally starting and stopping production to maximize the profits of a natural resource project. The optimal entry and exit from investment projects was also considered by [11] in another classical real option paper. A collection of illustrative real option papers can be found in [12].

In particular, we consider a firm contemplating the option to invest in an ethanol from corn production plant. We build on the analysis of our past work [23] which intended to quantify the impact (both intended and unintended consequences) of ethanol policy on production. This current work adds the complication of policy uncertainty deriving from a volumetric production tax subsidy which has changed several times over the past 35 years. We aim to understand the effects of ethanol policy uncertainty on production from the producer's perspective. An example of

the application of real option analysis to understand the effects of windfall taxes on mining operations can be found in [33]. A complementary and interesting analysis on policy uncertainty and real options can be found in [17]. The authors of [17] use empirical data to determine how regulatory uncertainty in American electricity markets affects start up and shut down decisions for power plants; their evidence supports the anecdotal claims mentioned above that uncertainty leads management to defer decision making. Our real option model sets out to design a framework to quantitatively model this added uncertainty and capture its effects on decision making.

1.1 Corn Ethanol Production and Subsidy Policy

The ethanol market in the US is large, estimated at 13.3 billion gallons produced in 2012 by over 209 plants [32]. Efforts to promote US energy independence and initiatives to obtain fuel from environmentally friendly sources have led to the subsidization of the production of ethanol biofuel from corn. Subsidies have historically been provided to ethanol producers by means of a volumetric ethanol excise tax credit for blenders and a small ethanol producer tax credit. The subsidy amount has changed from $0.40/gallon at its introduction in 1978 (Energy Tax Act) and been adjusted several times until its final level $0.45/gallon in the 2008 Farm Bill followed by termination (by non-renewal) at the end of 2012 [13, 15]. Table 1 shows the history of ethanol subsidy policy changes and amendments since its inception.

A year following the lapse of many of the energy subsidies, about one quarter of Nebraska's ethanol plants were in idle status [27]. The loss of the subsidy was a possible contributing factor to the shut downs as [21] note that, without subsidies, ethanol plants may lose their economic viability.

Table 1 Historical ethanol subsidies. Source: [15]

Act	Year	Subsidy ($/gallon)
Energy tax act	1978	0.40
Surface transportation assistance act of 1982	1983	0.50
Tax reform act	1984	0.60
Omnibus budget reconciliation act	1990	0.54
1998 policy adjustment effective 2001	2001	0.53
1998 policy adjustment effective 2003	2003	0.52
Extension of policy with adjustment	2005	0.51
Farm bill	2008	0.45
Expiration of tax credit	2012	–

1.2 Outline

Our paper uses a crush spread analysis to value a facility which produces ethanol from corn using a real options analysis following our framework in [23]. The outline is as follows: Section 2 specifies the plant characteristics, management decisions, and associated costs and profits. Section 3 derives the stochastic optimal control problem for the optimal plant operating rule. Section 4 illustrates the numerical results. Finally Sect. 5 draws conclusions about policy uncertainty and its effects on ethanol production, closing off with some policy recommendations.

2 The Real Option Model

Management contemplating the decision to invest in an ethanol production plant has the flexibility to enter or defer the project given price conditions and expected future profitability [12]. After initiating and building the ethanol plant, management again has the flexibility to switch production on (1) and off (0) given prevailing economic conditions. The goal of this paper is to examine how ethanol price and policy uncertainty affects a producer's business entry and subsequent operating decisions given price conditions, subsidy policy expectations, and the remaining project life.

Following our analysis [23], throughout this paper all currency is in United States dollars (USD); liquid volume is in gallons; solid volume is in bushels; weight is in tons; and interest is percent per year appropriate to USD deposits continuously compounded.

2.1 Plant Specification and Operating Costs

The following costs are scaled in terms of gallon of production capacity per year and were estimated by [34]. The model is based on our detailed ethanol real option analysis in [23]. This valuation considers the income stream associated with the production of ethanol from corn along with the ethanol-gasoline blender subsidy.

The capitalized construction cost B is estimated at \$1.40/gallon for a "typical" sized facility with nameplate capacity of 40,000,000 gallons/year. The plant salvage value Q is estimated at 10 % of capitalized cost. The switching cost D_{01} to resume production from an idle state is estimated at 10 % of capitalized cost per gallon of annual production capacity. Similarly, the switching cost D_{10} to pause production from an active operating state is estimated at 5 % of capitalized cost per gallon of annual production capacity.

2.2 Running Profits

The plant produces ethanol L_t (priced in USD/gallon) from corn C_t (priced in USD/bushel). The running profit from the corn ethanol crush spread is developed in [23] on a per bushel per year basis assuming the popular dry grind process for producing ethanol [4].

$$\text{corn} \rightarrow \text{ethanol} + \text{by-products} \tag{1}$$

The profit function while operating, f_1, is given by

$$f_1(L_t, C_t, Z_t) = \kappa(L_t + Z_t - K_1) - C_t \tag{2}$$

where Z_t is the government volumetric subsidy (USD/gallon). The conversion factor $\kappa = 2.8$ is the yield in terms of gallons of ethanol produced per bushel of corn [4] and is consistent with the CME Group's references on trading ethanol crush spreads [8].

The net running cost while on can be decomposed in terms of the fixed running cost p of \$0.68/gallon, less the average by-product distillers dried grains G (USD/ton) produced per bushel of corn [21, 23, 34]

$$K_1 = p - \frac{\omega}{\kappa} G. \tag{3}$$

The process produces 17 lbs of by-product per bushel and hence the yield factor $\omega = 17/2000$ [4].[1]

While production is idle, [34] estimated that fixed running costs K_0 are roughly 1 % of capitalized construction costs per gallon of production capacity or 20 % of fixed running cost while in production (note that, while idle, no ethanol is produced and consequently no subsidy is applied). The profit function while off, f_0, is

$$f_0(L_t, C_t, Z_t) = -\kappa K_0 \tag{4}$$

where the midpoint between the two estimates is used [23]

$$K_0 = \frac{0.01B + 0.20p}{2}. \tag{5}$$

Finally, the interest rate r is taken to be a target return of 8 % per annum continuously compounded to capture the risk associated with the ethanol project cash flows [23, 34]. Our analysis uses only the physical measure for the stochastic assets. We note however that the price risk associated with corn and ethanol can

[1] There are 2000 lbs in a ton.

be hedged using futures and the arbitrage free return can be determined by noting that the jumps are not correlated with the market following an argument popularized in [25].

2.3 Stochastic Price Models

Following our analysis in [23], ethanol L_t and corn C_t are modelled by a joint geometric Brownian motion (GBM) diffusion

$$dL_t = \mu L_t dt + \sigma L_t dW_{1t} \tag{6}$$

$$dC_t = aC_t dt + bC_t dW_{2t} \tag{7}$$

$$\text{Corr}[W_{1t}, W_{2t}] = \rho \tag{8}$$

where (W_{1t}, W_{2t}) is a two-dimensional Brownian motion defined on a filtered probability space $(\Omega, \mathscr{F}_t, P)$ which satisfies the usual conditions [28].

The econometric model parameters are estimated by ordinary least-squares regression of the log time series $\ln \frac{X_t}{X_{t-1}}$ using the 10 year monthly historical price series from Dec/02-Jan/11 capitalizing on earlier work in [23]. Prices for no. 2 yellow corn Omaha, NE underlying the CME corn futures contract were obtained from [36]. Average rack prices freight on board for ethanol were obtained from [26]. The correlation estimate ρ was obtained via the sample correlation of the residuals. Parameter estimation results are in Table 2. Note that both drifts were found to be statistically zero at the 95 % confidence interval. The estimate for the average distillers dried grains price $\hat{G}$ was estimated by regressing the time series against a constant.

The stochastic subsidy Z_t is modelled as a pure Poisson arrival time jump process with arrival rate λ and jumps of size J.

$$dZ_t = (J - Z_t)dN_t \tag{9}$$

Table 2 Regression estimation results

Parameter estimate	Value	t-test
$\hat{\mu}$	0	$P\left(\frac{\hat{\mu}-\mu}{s.e.} > t \middle\| \mu = 0\right) = 0.409$
$\hat{\sigma}$	0.156	–
$\hat{a}$	0	$P\left(\frac{\hat{a}-a}{s.e.} > t \middle\| \mu = 0\right) = 0.202$
$\hat{b}$	0.123	–
$\hat{\rho}$	0.105	–
$\hat{G}$	\$115.6	$G \in [108.4, 122.8]$[a]

[a] based on 95 % confidence interval Student-t with 119 degrees of freedom

Table 3 Maximum likelihood estimation results

Parameter estimate	Estimator	Value	95 % confidence interval
$\hat{\lambda}$	$\left(\frac{1}{n}\sum_{i=1}^{n} t_i - t_{i-1}\right)^{-1}$	0.24	[0.10, 0.42]
$\hat{\alpha}$	$\frac{1}{n}\sum_{i=1}^{n} \ln x_i$	−0.69	[−0.79, −0.58]
$\hat{\beta}^2$	$\frac{1}{n-1}\sum_{i=1}^{n} (\ln x_i - \hat{\alpha})^2$	0.015[a]	[0.0066, 0.062]

[a] Corrected unbiased estimator

where dN_t, defined on the probability space, is a continuous-time counting process $\{N_t, t \geq 0\}$ that counts the number of jumps over time dt and

$$dN_t = \begin{cases} 1 & \text{with probability } \lambda dt \\ 0 & \text{otherwise.} \end{cases} \tag{10}$$

The times between jumps $t_i - t_{i-1}$ are seen to be quite well modelled by independently exponentially distributed Poisson arrivals. The jumps J are assumed to be drawn from a lognormal distribution with parameters $LogN(\alpha, \beta^2)$. The parameters are estimated via maximum likelihood using the data in Table 1. The estimation results are summarized in Table 3.

The sample set for the subsidy policy is small (8 observations) and requires a test of the goodness of fit. By our model choice, the time between arrivals Δt of subsidy changes is exponentially distributed with parameter λ ($Exp(\lambda)$) and the series $\frac{\ln Z_t - \hat{\alpha}}{\hat{\beta}}$ has a Student's t-distribution since $\ln Z_t \sim N(\alpha, \beta^2)$. The plots of the estimated theoretical cumulative distribution functions (CDFs) versus the empirical distributions are included in Fig. 1 along with the QQ plots. By visual inspection, both data appear to be well suited to the proposed subsidy model.

Lilliefors tests (a nonparametric variant of the Kolmogorov-Smirnoff test) were applied to test for normality in the log subsidy series and exponentiality in the subsidy arrival times using MATLAB's `lilliefors.m` function. Both samples accepted the null hypothesis of normality and exponentiality at the 5 % significance level. This statistical evidence further supports our proposed model.

2.4 Policy Uncertainty "at its Worst"

Since the policy uncertainty cannot be hedged and is presumably not correlated with any market assets, there is cause for concern in terms of how to price this ethanol real option. Not only is there risk in the randomness of the process, but there is an

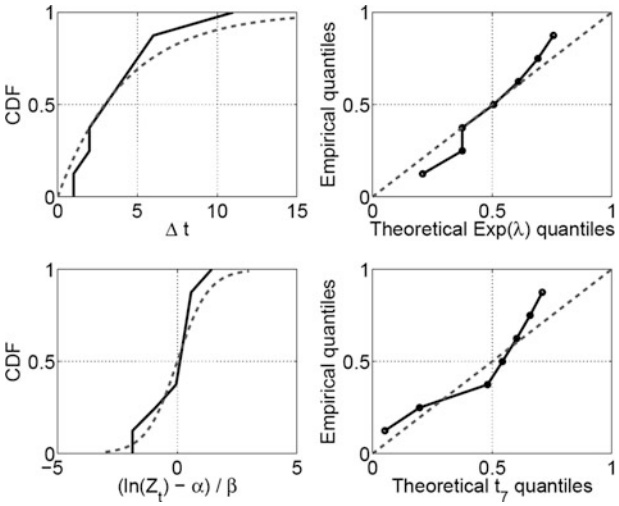

Fig. 1 The empirical CDF (*solid black*) vs the theoretical CDF (*grey dashed*) of the time between arrivals $\Delta t \sim Exp(\hat{\lambda})$ (*upper left*). The QQ plot of the time between arrivals (*upper right*). The empirical CDF (*solid black*) vs the theoretical CDF (*grey dashed*) of the normalized subsidy series $\frac{\ln Z_t - \hat{\alpha}}{\hat{\beta}} \sim t_7$ (*lower left*). The QQ plot of the subsidy series (*lower right*)

added complexity of uncertainty risk in the choice of model so-called "Knightian" uncertainty. To account for this model risk, uncertainty around the jump process parameters is included.

There are several possible ways to deal with model uncertainty and market incompleteness including: (1) cautiously deploying assumptions to simplify the problem; (2) utility indifference pricing with model uncertainty [19, 22]; and (3) best/worst case pricing (similar to the idea of good deal bounds and super-replication) [2]. Our analysis follows alternative (3) due to its financial intuition, transparency, and lack of subjectivity around economic aversion parameters or choice utility functions associated with utility-based pricing (which produce a subjective "personal price"). There is a connection between (2) and (3) however, in that as the risk aversion parameter tends to infinity, the utility indifference price tends to the worst-case price. Management buying into an ethanol project can be considered "long" the real option. The worst case price is what a strongly risk averse buyer may consider when purchasing an option.

Management contemplating investment in an ethanol project may ask the question: *Given the uncertainty around subsidy policy over the past 35 years, what is the expected case and worst case project value?* To answer this question, the reference policy uncertainty distribution is adjusted within the following heuristically determined parameter bounds to form best and worst case bounds for the project value.

2.4.1 Bounds on α

Suppose management assumes VaR_{05} style bounds on α.[2] In order to choose a lower bound for α, management chooses a parameter α_{min} such that the probability of observing a subsidy level J lower than the lowest historical subsidy $Z_{min} = 0.40$ is 95 %, i.e. $P(J < Z_{min}) = 0.95$. For a lognormal distribution with variance $\beta^2 = 0.015$, $\alpha_{min} = -1.118$. An upper bound can be chosen as α_{max} such that the probability of observing a lower subsidy J than the historical maximum $Z_{max} = 0.60$ is also less than 5 %, i.e. $P(J < Z_{max}) = 0.05$. In this case, the upper bound is $\alpha_{max} = -0.309$.[3]

2.4.2 Bounds on λ

Similarly, the average arrival time of subsidy changes is bounded by infinity (i.e. no changes at all) where $\lambda_{min} = 0$. Reasoning that the US Farm Bill is the primary means by which ethanol subsidy policies are amended and that a new omnibus bill is passed every 5 years or so, λ_{max} can be chosen such that the probability of observing at least one jump in a 5 year cycle is at least 95 %. Thus management seeks λ_{max} such that $P(k = 0; \lambda_{max}, t = 5) \leq 0.05$ (i.e. the probability of observing zero jumps is at most 5 %) where the probability of exactly k jumps occurring over t is $P(k; \lambda, t) = \frac{(\lambda t)^n}{n!} e^{-\lambda t}$. This is given by $e^{-\lambda_{max} 5} \leq 0.05 \Rightarrow \lambda_{max} = \frac{\ln(0.05)}{5}$ or $\lambda_{max} = 0.60$.

2.4.3 The Best and Worst Case Bounds

The best and worst case bounds can be summarized by the following:

$$\alpha \in [\alpha_{min}, \alpha_{max}] = [-1.118, -0.309] \tag{11}$$

$$\lambda \in [\lambda_{min}, \lambda_{max}] = [0, 0.60]. \tag{12}$$

[2]We note that management could use another technique to choose bounds such as the 95 % confidence intervals on the mean estimate for example in Table 3.

[3]We note that these bounds were chosen heuristically based on ethanol policy history and with reference to political precedent of the subsidy level. They do not represent a rigorous mathematical treatment of the small sample population time series.

3 The Stochastic Control Problem

In this section, we develop the jump diffusion counterpart of our model in [23] which leads to a system of interconnected obstacle problems, i.e. partial integro differential (PID) variational inequalities.

The total expected earnings V_i over the life of the project is given by the sum of its profits, plus the sum of any switching costs incurred over its operating life

$$V_i(l,c,z,t) = \sup_{\tau,u} E\left[\int_t^T e^{-r(s-t)} f_{I_s}(L_s,C_s,Z_s)ds + \sum_{k=1}^{n} e^{-r(\tau_k-t)} D_{u_{k-1},u_k} \middle| (L_t,C_t,Z_t,u_0) = (l,c,z,i)\right] \tag{13}$$

The pair (τ, u) is the control that the manager has over the facility in his ability to toggle production on and off. It consists of a set of switching times τ_k and states to be switched into u_k with $I_t = u_k, t \in [\tau_k, \tau_{k+1})$. Thus τ_k is an increasing set of switching times with $\tau_k \in [t,T]$ and $\tau_k < \tau_{k+1}$ given the initial operating state $u_0 = i$.

If management assumes a worst case pricing scenario for the policy parameters (λ, α), then

$$V_i(l,c,z,t) = \sup_{\tau,u} \inf_{\lambda,\alpha} E\left[\int_t^T e^{-r(s-t)} f_{I_s}(L_s,C_s,Z_s)ds + \sum_{k=1}^{n} e^{-r(\tau_k-t)} D_{u_{k-1},u_k} \middle| (L_t,C_t,Z_t,u_0) = (l,c,z,i)\right] \tag{14}$$

where $\lambda \in [\lambda_{min}, \lambda_{max}]$ and $\alpha \in [\alpha_{min}, \alpha_{max}]$. The limits on λ and α prevent the optimization argument from growing unbounded and becoming singular [29]. The controls $(u, \tau, \alpha, \lambda)$ come from an admissible set of non-anticipating controls (i.e. $\mathscr{F}_t$-measurable and Markovian).

3.1 An Intuition Building One-Dimensional Simplified Model

To make the full model exposition easier and to develop intuition consider, for the time being, a simplified one-dimensional approximation of the spread less fixed running costs

$$X_t = \kappa L_t - C_t - K \tag{15}$$

where X_t follows a simple Brownian stochastic differential equation

$$dX_t = adt + bdW_t \tag{16}$$

where a and b are naively chosen to fit the model. To further simplify the process, assume now that Z_t has normally distributed jumps such that

$$dZ_t = JdN_t \tag{17}$$

where $J \sim N(\alpha, \beta^2)$. The two $(X_t + Z_t)$ can be combined into a jump diffusion process Y_t

$$dY_t = adt + bdW_t + JdN_t \tag{18}$$

with solution

$$Y_t = Y_0 + at + bW_t + \sum_{k=1}^{n} J_k \tag{19}$$

where $\sum_{k=1}^{n} J_k \sim N(n\alpha, n\beta^2)$.

The expected income of the facility over its lifespan is

$$V_i(y,t) = \sup_{\tau,u} \inf_{\lambda,\alpha} E\left[\int_t^T e^{-r(s-t)} f_{I_s}(Y_s) ds + \sum_{k=1}^{n} e^{-r(\tau_k - t)} D_{u_{k-1},u_k} \,\middle|\, (Y_t, u_0) = (y,i) \right] \tag{20}$$

By application of dynamic programming (see [5] or [29]) for optimal switching problems, the value function can be written as

$$V_i(y,t) = \sup_{\tau} \inf_{\lambda,\alpha} E\left[\int_t^\tau e^{-r(s-t)} f_i(Y_s) ds + e^{-r(\tau - t)} \left\{ V_j(Y_\tau, \tau) - D_{ij} \right\} \right] \tag{21}$$

where $i, j \in \{0, 1\}$ and τ is the first time it is optimal to switch production regimes. Now the problem consists of finding the optimal sets of prices and times to either

- hold production in its current state i, denoting this continuation or (hold) set as H_i, or
- switch production into the other state j, denoting this switching set as S_{ij}.

By another application of dynamic programming and Ito's lemma for jump diffusions, this equation leads to a coupled system of free boundary PID equations (PIDEs). The free boundary problem can be written in complementary form by noting that either it is optimal to switch and $V_i = V_j - D_{ij}$ or it is optimal to hold and V_i satisfies a PIDE subject to $V_i \geq V_j - D_{ij}$. Thus the equation extends on the whole space easing the need to track the switching boundary as a PID variational inequality (see [28] for an excellent reference on controlled jump diffusions). Thus the system of equations may be expressed as

$$\max \left[\underbrace{\frac{\partial V_i}{\partial t} + \mathscr{L}[V_i] + \inf_{\lambda,\alpha} \mathscr{I}[V_i] + f_i - rV_i}_{H_i}, \quad \underbrace{(V_j - D_{ij}) - V_i}_{S_{ij}} \right] = 0. \tag{22}$$

where the spatial differential part of the generator is

$$\mathscr{L}[V] = a\frac{\partial V}{\partial y} + \frac{1}{2}b^2\frac{\partial^2 V}{\partial y^2} \tag{23}$$

and the integro part is

$$\mathscr{I}[V] = \lambda(E[V(y+J)] - V(y)). \tag{24}$$

The expectation E is taken with respect to a normal $N(\alpha, \beta^2)$ kernel g_N

$$E[V(y+J)] = \int_{-\infty}^{\infty} V(y+J)g_N(J)dJ. \tag{25}$$

Theorem 1 (Worst Case Price). *The minimal optimal control is given by*

$$\alpha = \alpha_{min}, \;\; \lambda = \begin{cases} \lambda_{min} & \text{if } E[V(y+J)] - V(y) \geq 0, \\ \lambda_{max} & \text{if } E[V(y+J)] - V(y) < 0 \end{cases} \tag{26}$$

Theorem 2 (Best Case Price). *The maximal optimal control is given by*

$$\alpha = \alpha_{max}, \;\; \lambda = \begin{cases} \lambda_{max} & \text{if } E[V(y+J)] - V(y) \geq 0, \\ \lambda_{min} & \text{if } E[V(y+J)] - V(y) < 0 \end{cases} \tag{27}$$

Theorem 3 (Worst and Best Case Price if $\alpha = 0$). *The minimal optimal control is given by*

$$\lambda = \lambda_{min}, \tag{28}$$

and the maximal optimal control is given by

$$\lambda = \lambda_{max}, \tag{29}$$

if $\alpha = 0$ for all y.

See Appendix 2 for proofs of the above.

An interpretation of the maximal (respectively minimal) optimal control is as follows: (1) If the expected value post-jump $E[V(y+J)]$ is better than its current value $V(y)$, assume that the jump arrives as (in)frequently as possible $1/\lambda_{max}$ $(1/\lambda_{min})$. (2) Assume that the jumps are in general as (un)favourable as possible α_{max} (α_{min}).

3.1.1 Lessons from Merton

In the simplification where (1) the policy parameters (λ, α) are constant and (2) switching costs D_{ij} are zero, the problem reduces to a PIDE which yields the option price

$$\frac{\partial V}{\partial t} + a\frac{\partial V}{\partial y} + \frac{1}{2}b^2\frac{\partial^2 V}{\partial y^2} + \lambda(E[V(y+J)] - V(y)) - rV + f(y) = 0 \tag{30}$$

where $f(y) = y^+ = \max(y, 0)$.

Using the Feynman-Kac Formula [28] and following Merton's classical paper on jump diffusions [25], the solution to the PIDE is

$$V(y,t) = E\left[\int_t^T e^{-r(s-t)} f(Y_s) ds \,\middle|\, Y_t = y\right]. \tag{31}$$

Theorem 4 (Constant Coefficient Option Price). *The option price $V(y,t)$ satisfies*

$$V(y,t) = \sum_{n=0}^{\infty} \int_t^T e^{-\lambda(s-t)} \frac{\lambda^n (s-t)^n}{n!} e^{-r(s-t)} \left(A_{s,n}\Phi(d) + \frac{B_{s,n}}{\sqrt{2\pi}} e^{-\frac{d^2}{2}} \right) ds \tag{32}$$

where $A_{s,n} = y + a(s-t) + n\alpha$, $B_{s,n}^2 = b^2(s-t) + n\beta^2$, $d = A_{s,n}/B_{s,n}$ and $\Phi(x)$ is the standard normal cumulative distribution function.

See Appendix 2 for the derivation of the governing PIDE and option price.

3.2 The Complete Problem

Return now to the stochastic control problem for the real option

$$\begin{aligned} V_i(l,c,z,t) = \sup_{\tau,u} \inf_{\lambda,\alpha} E\Bigg[& \int_t^T e^{-r(s-t)} f_{I_s}(L_s, C_s, Z_s) ds \\ & + \sum_{k=1}^{n} e^{-r(\tau_k - t)} D_{u_{k-1},u_k} \,\Bigg|\, (L_t, C_t, Z_t, u_0) = (l,c,z,i) \Bigg] \end{aligned} \tag{33}$$

where $\lambda \in [\lambda_{min}, \lambda_{max}]$ and $\alpha \in [\alpha_{min}, \alpha_{max}]$. We follow a similar argument as before using dynamic programming to reduce the switching problem to a single decision τ

$$\begin{aligned} & V_i(l,c,z,t) \\ & = \sup_{\tau} \inf_{\lambda,\alpha} E\left[\int_t^{\tau} e^{-r(s-t)} f_i(L_s, C_s, Z_s) ds + e^{-r(\tau-t)} \{V_j(L_\tau, C_\tau, Z_\tau, \tau) - D_{ij}\} \right]. \end{aligned} \tag{34}$$

Using Ito's lemma for jump diffusions and noting as in [5, 29, 37] that the problem can be written in complementary form as a variational inequality

$$\max\left[\underbrace{\frac{\partial V_i}{\partial t}+\mathscr{L}[V_i]+\inf_{\lambda,\alpha}\mathscr{I}[V_i]+f_i-rV_i}_{H_i},\ \underbrace{(V_j-D_{ij})-V_i}_{S_{ij}}\right]=0. \tag{35}$$

where the spatial differential part of the generator is

$$\mathscr{L}[V]=\mu l\frac{\partial V}{\partial l}+ac\frac{\partial V}{\partial c}+\frac{1}{2}\sigma^2l^2\frac{\partial^2V}{\partial l^2}+\rho\sigma lbc\frac{\partial^2V}{\partial l\partial c}+\frac{1}{2}b^2c^2\frac{\partial^2V}{\partial c^2} \tag{36}$$

and the integro part is

$$\mathscr{I}[V]=\lambda(E[V(l,c,J)]-V(l,c,z)). \tag{37}$$

Theorem 5 (Worst Case Price). *The minimal optimal control is given by*

$$\alpha=\alpha_{min},\ \ \lambda=\begin{cases}\lambda_{min} & \text{if } E[V(l,c,J)]-V(l,c,z)\geq 0,\\ \lambda_{max} & \text{if } E[V(l,c,J)]-V(l,c,z)<0\end{cases} \tag{38}$$

Theorem 6 (Best Case Price). *The maximal optimal control is given by*

$$\alpha=\alpha_{max},\ \ \lambda=\begin{cases}\lambda_{max} & \text{if } E[V(l,c,J)]-V(l,c,z)\geq 0,\\ \lambda_{min} & \text{if } E[V(l,c,J)]-V(l,c,z)<0\end{cases} \tag{39}$$

See Appendix 2 for proofs of the above.

3.3 The Decision to Enter

Management's optimal decision time to enter into the business τ maximizes the expected value

$$V(l,c,z,t)=\sup_{\tau}\inf_{\lambda,\alpha}E\left[e^{-r(\tau-t)}\max\{V_1,V_0\}(L_\tau,C_\tau,Z_\tau,\tau)-B\middle|\,(L_t,C_t,Z_t)=(l,c,z)\right] \tag{40}$$

and is a classical "American" style exercise call option. By dynamic programming, the optimal stopping problem satisfies the PID variational inequality

$$\max\left[\underbrace{\frac{\partial V}{\partial t}+\mathscr{L}[V]+\inf_{\lambda,\alpha}\mathscr{I}[V]-rV,}_{H}\quad\underbrace{(\max(V_1,V_0)-B)-V}_{S}\right]=0. \tag{41}$$

This completes the jump diffusion analogue of [23] and represents the optimal entry strategy for investment into a corn-ethanol biofuel production plant.

4 Numerical Results

This section begins with a numerical investigation of the behaviour of the constant coefficient analytical model. The section then proceeds with an investigation of the effects of policy uncertainty on the one-dimensional model including (i) the loss in value and (ii) the effects on switching decisions (which is also a proxy investigation of the effects on the entry decision). Finally, the section concludes with an investigation of the change in value between the full model with both policy uncertainty and model certainty or uncertainty.

4.1 The Constant Coefficient Model

Consider $V(y,t)$ in Eq. 32. Its behaviour is monotone increasing in y. Figure 2 shows that the function is increasing in α. This is as expected since if the jumps tend to be more positive ($\alpha > 0$), the spread tends to jump non-locally to a higher value of y (recall the option is monotone increasing in y), and vice versa if α tends to be more negative.

Figure 3 indicates V is an increasing function of λ (although it is generally insensitive to λ). This makes sense intuitively since as the frequency of jumps increases, more volatility is added to the option in terms of $B_{s,n}$, and Black-Scholes style options are increasing functions in volatility.

Figure 4 shows that V is sensitive to λ when there is an expected direction with the jumps (i.e. $\alpha \neq 0$).

4.1.1 Impact on Value

The parameters λ and α can be interpreted as measures of how infrequently policy changes occur and where management expects the subsidy to level move to, respectively. If the subsidy is expected to move up in value $\alpha > 0$, the jumps make the project more favourable. The opposite occurs if $\alpha < 0$: The future policy outlook is negative, and the project/option loses value.

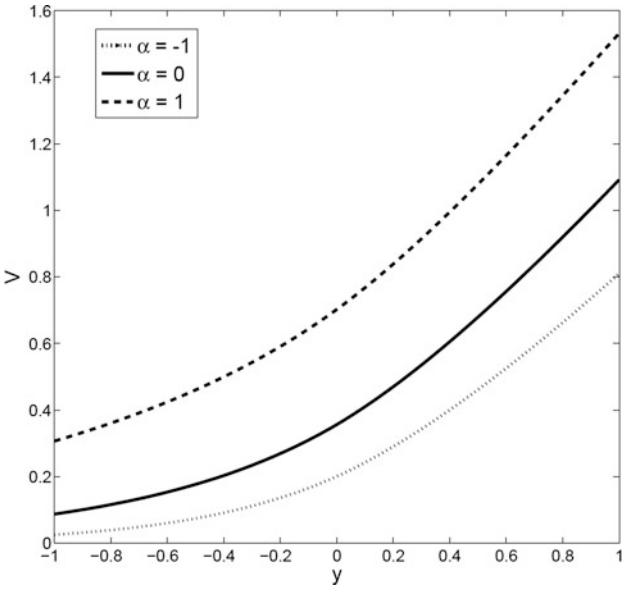

Fig. 2 The option value $V(y,t)$ at various levels of α (expected jump level) given standard parameters of $\lambda = 1$ (Poisson arrival rate of jumps), $\beta = 1$ (volatility of jump distribution), $a = 0$ and $b = 1$ (drift and volatility of diffusion), $r = 0.01$ (discount rate), and $T - t = 1$ (remaining option tenor)

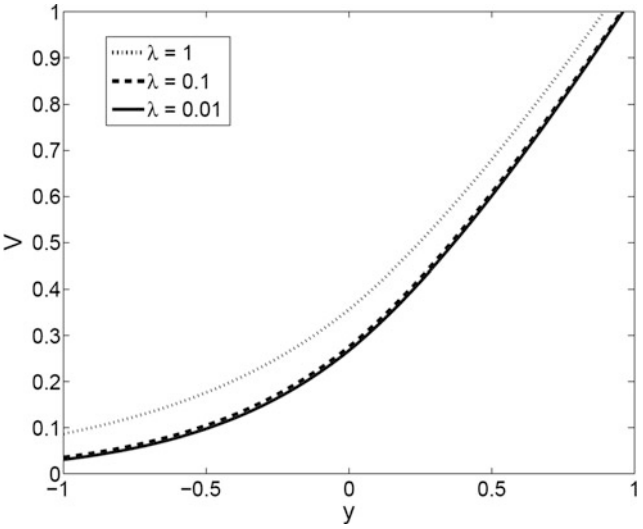

Fig. 3 The option value $V(y,t)$ at various levels of λ (Poisson arrival rate of jumps) given standard parameters of $\alpha = 0$ (expected jump level), $\beta = 1$ (volatility of jump distribution), $a = 0$ and $b = 1$ (drift and volatility of diffusion), $r = 0.01$ (discount rate), and $T - t = 1$ (remaining option tenor)

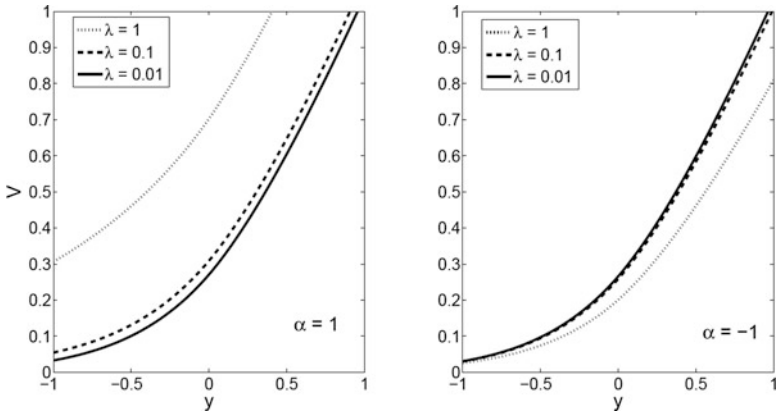

Fig. 4 The option value $V(y,t)$ at various levels of λ (Poisson arrival rate of jumps) and α (expected jump level) given standard parameters of $\beta = 1$ (volatility of jump distribution), $a = 0$ and $b = 1$ (drift and volatility of diffusion), $r = 0.01$ (discount rate), and $T - t = 1$ (remaining option tenor). *On the left*, $\alpha = 1$ and *on the right* $\alpha = -1$

As λ increases, policy changes occur more frequently which adds project/option value by means of the increased volatility associated with each jump. As the option to switch production off mitigates downside jumps on value V, the upside value of the jump volatility disproportionately increases the option's value. Figure 3 also reveals that the option is very insensitive to λ when there is no expected "directionality" in the jumps, i.e. when $\alpha = 0$.

4.2 The One-Dimensional Model

We now turn to an investigation of the effects of model uncertainty for a risk averse investor into the real option ethanol project. In this analysis, $f_1(y) = y$ and $f_0(y) = 0$ while $D_{01} = 0.2$ and $D_{10} = 0.1$.

Figure 5 shows the project valuation results for the expected price with policy uncertainty, best and worst case prices given policy uncertainty where $\alpha = 0$ is fixed and $\lambda \in [0, 1]$. The underlay shows the switching boundaries S_{ij} in y. Figure 6 shows the same information as Fig. 5 but in this case there is model uncertainty $\alpha \in [-0.2, 0.2]$ with expected parameter $\alpha = 0$.

4.2.1 Impact on Value

The gap between the best and worst case prices can be significantly large if α is allowed to vary indicated in Fig. 6; otherwise the difference is small (Fig. 5) as expected from our results with the constant coefficient model. Since this function is convex, the integral operator is single-signed and the parameter λ assumes either

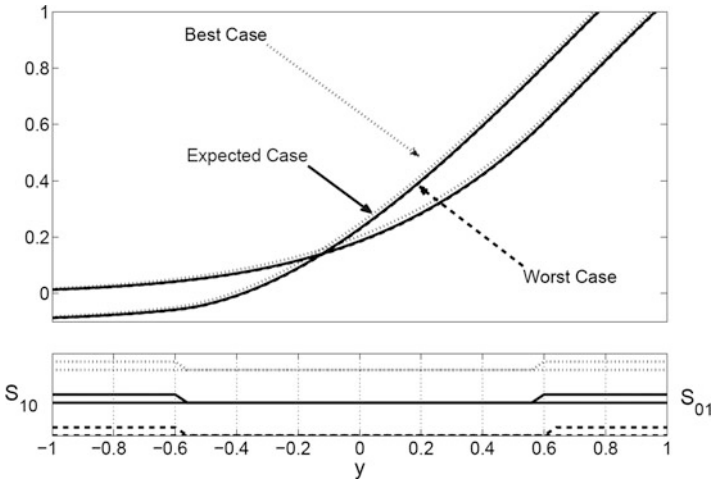

Fig. 5 The option value $V(y,t)$ at an "expected case" of $\lambda = 0.1$ (Poisson arrival rate of jumps) and $(\lambda_{min}, \lambda_{max}) = (0,1)$ (parameter boundaries), $\alpha = 0$ and $\beta^2 = 0.1$ (mean and variance of jump distribution), $a = 0$ and $b = 1$ (drift and volatility of diffusion), $r = 0.01$ (discount rate), and $T - t = 1$ (option tenor). Switching costs are $D_{01} = 0.2$ and $D_{10} = 0.1$

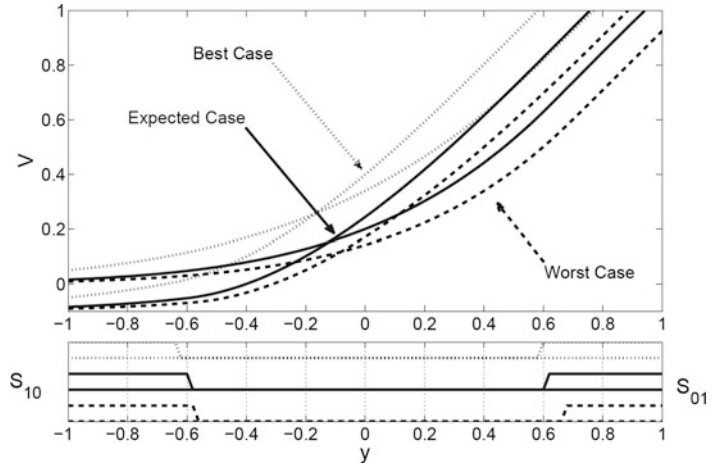

Fig. 6 The option value $V(y,t)$ at an "expected case" of $\lambda = 0.1$ (Poisson arrival rate of jumps) and $\alpha = 0$ (expected mean jump size), but where $\lambda \in [0,1]$ and $\alpha \in [-0.2, 0.2]$ (parameter boundaries). The remaining parameters are $\beta^2 = 0.1$ (variance of jump distribution), $a = 0$ and $b = 1$ (drift and volatility of diffusion), $r = 0.01$ (discount rate), and $T - t = 1$ (option tenor). Switching costs are $D_{01} = 0.2$ and $D_{10} = 0.1$

λ_{min} in the worst case or λ_{max} in the best case when $\alpha = 0$ in the example in Fig. 5 by Jensen's inequality. The constant coefficient expected case model will always be bounded by the best and worst case project prices. In these examples, the expected case is nearer to the worst case since $\lambda = 0.1$ is closer to $\lambda_{min} = 0$ than $\lambda_{max} = 1$.

4.2.2 Impact on Switching Decision

Although the effects are not very pronounced on the 1 year time horizon, model uncertainty has an impact on switching decisions. The lower charts in Figs. 5 and 6 represent the switching boundaries

- $S_{01} = \{y : V_0(y,0) = V_1(y,0) - D_{01}\}$, the set of prices where the operating status is optimally switched on from idle, and
- $S_{10} = \{y : V_1(y,0) = V_0(y,0) - D_{10}\}$, the set of prices where the operating status is optimally switched off from running.

It can be seen that in the...

...worst case scenario: The operator switches production on later than in the expected case (i.e. at $y > y^*$ if y^* is where the operator would switch production on in the expected case). Similarly, the operator switches production off earlier compared to the expected case (i.e. at $y < y^*$ if y^* is where the operator would switch production off in the expected case).

...best case scenario: The operator switches production on earlier and switches production off later compared to the expected case.

In the example where $\alpha = 0$ is fixed, the differences in switching boundaries between the best, worst and expected cases are almost negligible (Fig. 5). However in the other example where $-0.2 \leq \alpha \leq 0.2$ can vary, the differences in switching boundaries between the best, worst and expected cases can deviate a great deal. Thus it is not so much when management thinks a change in policy might occur (i.e. λ-driven) but rather how management expects that policy to change with respect to its current policy conditions—that is, α-driven.

4.3 The Complete Model

This section concludes with a numerical investigation of the ethanol plant value in the presence or absence of policy uncertainty and model uncertainty. The ethanol plant is assumed to have a 10 year investment horizon, $T - t = 10$.

4.3.1 With and Without Policy Uncertainty

We compare the real option project valuation of the ethanol plant in two cases where:

- Management ignores the uncertainty in the ethanol subsidy policy and assumes $Z_t = Z$ (constant) to take its Jan/2011 value (Table 1),
  - in this case, $f_1(L_s, C_s, Z) = \kappa(L_s - K_1 + Z) - C_s$ where $Z = \$0.45$/gallon is constant (also $\lambda = 0$); and

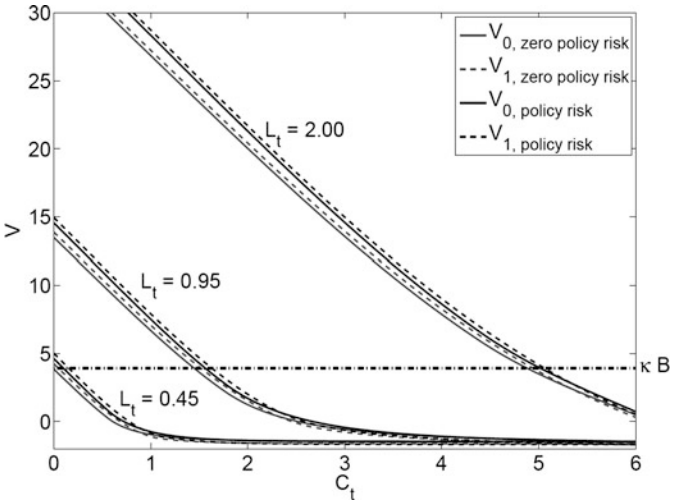

Fig. 7 $V(L_t, C_t, Z, t)$ without policy uncertainty vs $V(L_t, C_t, Z_t, t)$ with policy uncertainty. Parameters (from Tables 2 and 3) are $\mu = 0$ and $\sigma = 0.156$ (drift and volatility of ethanol), $a = 0$ and $b = 0.123$ (drift and volatility of corn), $Z = 0.45$ without policy uncertainty and $Z_t = 0.45$, $\lambda = 0.24$, $\alpha = -0.69$ and $\beta^2 = 0.015$ (arrival rate, mean and variance of jumps) with policy uncertainty

- Management considers the uncertainty in the ethanol subsidy policy with known parameters (model certainty) and assumes the model parameters in Table 3 subject to the initial subsidy level being its Jan/2011 value as above,
  - in this case, $f_1(L_s, C_s, Z_s) = \kappa(L_s - K_1 + Z_s) - C_s$ where $Z_t = \$0.45$/gallon.

Figure 7 shows the value functions at various levels of C_t in the presence and absence of policy uncertainty. Figure 8 shows the switching boundaries in both cases.

Impact of Policy Uncertainty on Value As inferred from our one-dimensional analysis in Sect. 3.1, policy uncertainty adds more value to the real option due to two distinct factors: (1) Given $Z_t = 0.45 < 0.51 = e^{\alpha + \frac{1}{2}\beta^2} = E[J]$, it is likely that the subsidy policy will jump to a higher level giving the option more value in the presence of policy uncertainty. (2) The extra volatility provided by the jump process adds volatility value to the option. The downside of policy switches on an ethanol plant can be mitigated by switching production off, while the upside value is maintained by keeping (or switching) production on when prices favourably allow for it. The capitalized cost of construction on a per bushel basis κB is also included in Fig. 8.

Impact of Policy Uncertainty on Switching Decisions The boundary at which production is switched on from an idle state is ∂S_{01} and the boundary at which production is turned off from a running state is ∂S_{10}. In this case, the initial subsidy

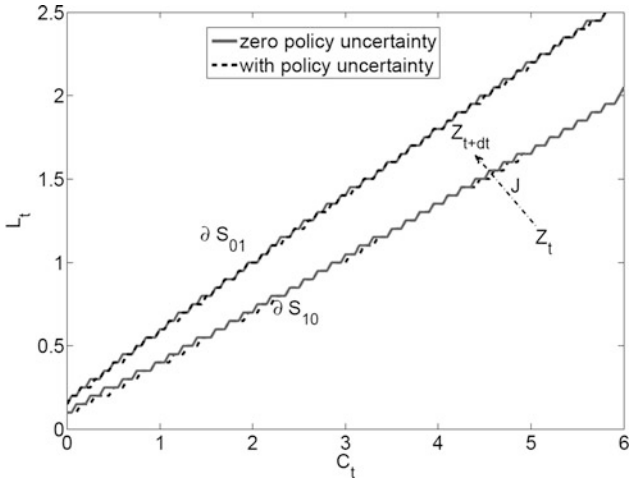

Fig. 8 The switching boundaries ∂S_{01} and ∂S_{10} in the presence and absence of policy uncertainty. Parameters (from Tables 2 and 3) are $\mu = 0$ and $\sigma = 0.156$ (drift and volatility of ethanol), $a = 0$ and $b = 0.123$ (drift and volatility of corn), $Z = 0.45$ without policy uncertainty and $Z_t = 0.45$, $\lambda = 0.24$, $\alpha = -0.69$ and $\beta^2 = 0.015$ (arrival rate, mean and variance of jumps) with policy uncertainty

level Z_t is less than the long run average $E[J] = e^{\alpha+\frac{1}{2}\beta^2}$, $Z_t = 0.45 < 0.51 = e^{-0.69+\frac{1}{2}0.015}$. Thus, the operator generally waits longer before turning production off, due to a positive outlook that the subsidy might jump up to its long term average. Similarly, the operator generally turns production on sooner in hope that the subsidy might again jump to its (higher) long run average. More precisely, given a point (c, l) on ∂S_{01} in the absence of policy uncertainty, if (c, l^*) is on ∂S_{01}^* in the presence of policy uncertainty, then $l^* < l$ (respectively $l^* > l$) when production is shut down earlier (later).

Changes in z shift value and switching decisions up or down non-locally as Z_t jumps. The general direction of the jumps is illustrated in Fig. 8 by the arrow $Z_t \xrightarrow{J} Z_{t+dt}$.

It should be noted that if management were expecting the subsidy to jump to a lower level, the opposite situation as described above would occur. Management would switch production off earlier and turn production on later for fear that the subsidy might fall.

4.3.2 Policy Uncertainty with Model Uncertainty

In the likely event that the distribution and parameters of the regulatory uncertainty process are unknown, management may choose a worst case valuation for the ethanol plant project value. The assumed boundaries for policy change arrival rate are $\lambda \in [0, 0.60]$ and expected mean subsidy policy $\alpha \in [-1.118, -0.309]$.

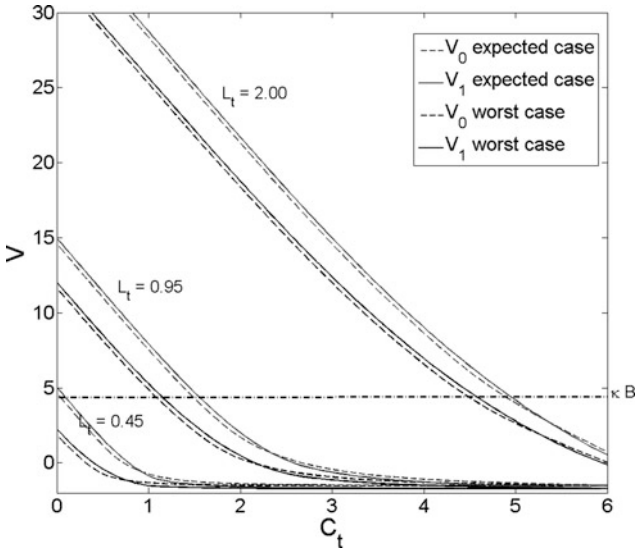

Fig. 9 $V(L_t, C_t, Z_t, t)$ vs $\inf_{\lambda,\alpha} V(L_t, C_t, Z_t, t)$ with policy (and model) uncertainty. Constant parameters (from Tables 2 and 3) are $\mu = 0$ and $\sigma = 0.156$ (drift and volatility of ethanol), $a = 0$ and $b = 0.123$ (drift and volatility of corn), and $Z_t = 0.45$, $\lambda = 0.24$, $\alpha = -0.69$ and $\beta^2 = 0.015$ (arrival rate, mean and variance of jumps). Non-constant parameters for model uncertainty are $\alpha \in [-1.118, -0.309]$ and $\lambda \in [0, 0.60]$

Figure 9 illustrates the worst case value compared to the expected case given by the model parameters in Tables 2 and 3. The switching boundaries are illustrated in Fig. 10 comparing the worst case operating decisions to the expected case.

For completeness, Fig. 11 shows the envelope of best case, worst case and expected project values in the presence of policy and model uncertainty. The bounds can be quite large between the best and worst project values even for "seemingly small" parameter boundaries. The switching boundaries are illustrated in Fig. 12 comparing the best case operating decisions to the expected case.

Impact of Worst Case Model Uncertainty on Value The worst case real option ethanol plant value represents a lower bound in project value. Figure 9 also includes the capitalized cost of construction on a per bushel of capacity basis κB. As expected, fewer projects are net present value positive in the worst case project value compared to the expected case. That is, given the two sets of prices at a time t the set of prices that are "Net Present Value (NPV) positive" for entering into the project are

$$NPV = \{(l, c) : \max(V_1, V_0) - B > 0\} \text{ and } NPV^* = \{(l, c) : \inf_{\lambda,\alpha} \max(V_1, V_0) - B > 0\}, \tag{42}$$

then

$$NPV^* \subseteq NPV \tag{43}$$

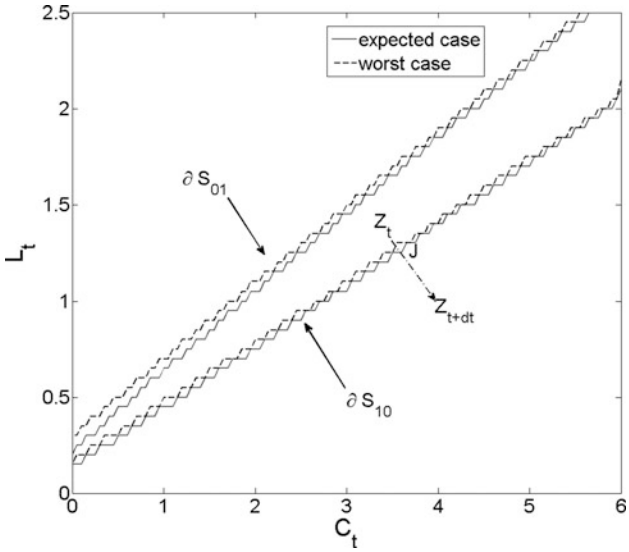

Fig. 10 The switching boundaries ∂S_{01} and ∂S_{10} in the presence of policy uncertainty and model uncertainty in the worst case. Constant parameters (from Tables 2 and 3) are $\mu = 0$ and $\sigma = 0.156$ (drift and volatility of ethanol), $a = 0$ and $b = 0.123$ (drift and volatility of corn), and $Z_t = 0.45$, $\lambda = 0.24$, $\alpha = -0.69$ and $\beta^2 = 0.015$ (arrival rate, mean and variance of jumps). Non-constant parameters for model uncertainty are $\alpha \in [-1.118, -0.309]$ and $\lambda \in [0, 0.60]$

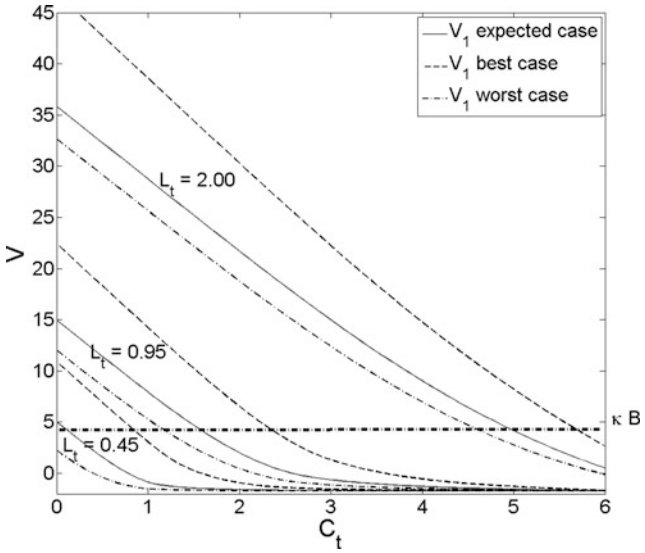

Fig. 11 $V_1(L_t, C_t, Z_t, t)$ vs $\inf_{\lambda,\alpha} V_1(L_t, C_t, Z_t, t)$ vs $\sup_{\lambda,\alpha} V_1(L_t, C_t, Z_t, t)$ with policy uncertainty. Constant parameters (from Tables 2 and 3) are $\mu = 0$ and $\sigma = 0.156$ (drift and volatility of ethanol), $a = 0$ and $b = 0.123$ (drift and volatility of corn), and $Z_t = 0.45$, $\lambda = 0.24$, $\alpha = -0.69$ and $\beta^2 = 0.015$ (arrival rate, mean and variance of jumps). Non-constant parameters for model uncertainty are $\alpha \in [-1.118, -0.309]$ and $\lambda \in [0, 0.60]$

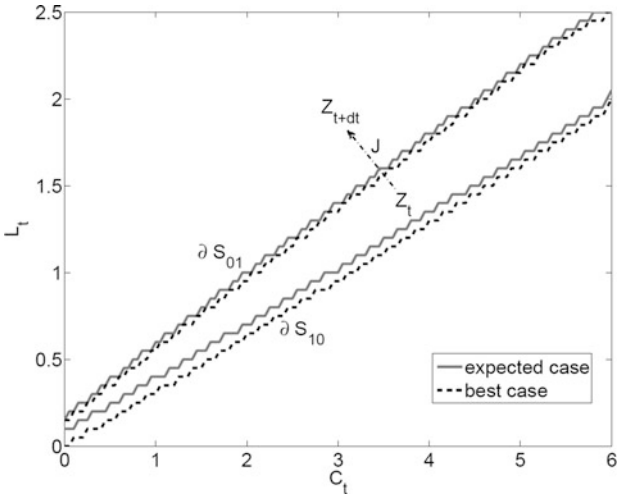

Fig. 12 The switching boundaries ∂S_{01} and ∂S_{10} in the presence of policy uncertainty and model uncertainty in the best case. Constant parameters (from Tables 2 and 3) are $\mu = 0$ and $\sigma = 0.156$ (drift and volatility of ethanol), $a = 0$ and $b = 0.123$ (drift and volatility of corn), and $Z_t = 0.45$, $\lambda = 0.24$, $\alpha = -0.69$ and $\beta^2 = 0.015$ (arrival rate, mean and variance of jumps). Non-constant parameters for model uncertainty are $\alpha \in [-1.118, -0.309]$ and $\lambda \in [0, 0.60]$

This means that fewer investments are entered into during times of high policy uncertainty if management is risk averse.

In certain cases, the integral operator may be $\mathscr{I}[V] = E[V(l, c, J)] - V(l, c, 0.45) > 0$ and accordingly $\lambda = \lambda_{min} = 0$ in the minimization. This is similar to the case with zero policy uncertainty. Thus, the worst case option value may at times approach the option value in the absence of policy uncertainty.

Impact of Worst Case Model Uncertainty on Operating Decisions The possible subsidy outcomes in the worst case scenario have a much more negative outlook than the expected case. Thus in the worst case scenario, the optimal strategy tends to be conservative when making switching decisions (Fig. 10). The net result is that management switches production on much later and switches production off much earlier compared to the expected case operating strategy.

Comments on the Best Case Model Figure 11 shows that the gap between the best and worst case prices can be quite large. This is an artifact of the stochastic optimization problem that leads to very large arbitrage free price good deal bounds in practice with financial derivatives. Similar to before, management switches production on earlier and switches production off later compared to the expected case operating strategy (Fig. 12).

5 Conclusions

The goal of our paper is to develop a quantitative model for managing and pricing regulatory risk. The accomplishments and overall theme of our paper are summarized in what follows.

5.1 Summary

Our paper laid out several research goals to contribute to the existing real options literature and the less developed body of research in policy uncertainty.

We presented a real option model to attempt to quantitatively model policy uncertainty using a jump diffusion process. This model allows for the valuation of long term energy projects in the presence of policy uncertainty. For a corn-ethanol case study (following [23]), we presented a real option model involving both standard price uncertainty modelled using a simplified one dimensional jump diffusion process for the relevant price spread and stochastic subsidy. We followed this with a more sophisticated multivariate model which independently modeled both the input and the output price. In addition, this model included the impact of policy uncertainty using a randomly fluctuating subsidy level. This fluctuating subsidy was quantified using a pure jump process. Given that there may be model uncertainty for the subsidy policy process, our proposed model includes a "worst case" (modelled using a *VaR* level) policy uncertainty scenario which allows the project investor to quantify and manage his worst case regulatory downside risk. This work allowed us to draw some general conclusions with policy level implications, as summarized and described in the next section.

5.2 Policy Conclusions

We outline the policy effects and numerical conclusions from our analysis in Sect. 4.

5.2.1 Policy Uncertainty

In the case of policy certainty versus uncertainty, for the convex (or "long vol") real options considered here, the effects of policy uncertainty always increase the value of the option when there is no directionality in the subsidy jumps.

More generally, the effects of policy uncertainty may be positive or negative for the project valuation. For example, if the subsidy is currently low and the future subsidy level is expected to be higher, the possibility of a jump in policy increases the overall value of the option. The opposite holds when the subsidy is high and the future subsidy is expected to be lower than today.

5.2.2 Model Uncertainty

Typically, the effect of ambiguity in policy uncertainty models on project valuation is negative: A strongly risk averse manager taking a long position in the option should price the project using the worst case of possible parameters.

The optimal operating strategy in terms of the sets of prices, times, and subsidy levels to switch production vary based on the scenario. The strategy however generally obeys the following rules: (1) If the scenario is a worst case (respectively best case), then production is switched off earlier (later) compared to the constant parameter expected case, and production is switched on later (earlier) compared to the expected case. This represents an pessimistic (optimistic) outlook on regulatory policy changes. (2) If the scenario is a constant parameter case with policy uncertainty, then production is switched on earlier (later) if the current policy regime is lower (higher) than the expected long run trend. Similarly production is switched off later (earlier) if the current policy regime is lower (higher) than the expected long run trend.

The anecdotal evidence that suggests businesses delay investment longer in periods of high policy uncertainty is seen to be consistent with our model, supporting those claims [3, 17, 35]. In particular, given the tendency is generally to delay during periods of policy uncertainty suggests that investors use pessimistic model outlooks when making investment decisions. Given that fewer projects were net present value positive in the model uncertainty case versus the policy uncertainty with known parameters case, our model supports the claim that fewer investments are entered into during periods of high policy uncertainty.

5.3 Possible Extensions

The lognormal distribution for the policy subsidy jump process was chosen for several reasons: (1) subsidies cannot become negative; (2) model familiarity, since geometric Brownian motion itself leads to a lognormal distribution and Merton's seminal jump diffusion paper [25]; (3) analytical tractability; and (4) its second moments exist. The distribution however has large positive skew with a fat tail. This choice of distribution can lead to results which are relatively indifferent toward downside risk in the subsidy process, as the probability of observing very low subsidies is much smaller than the probability of observing very high subsidies. For reference, plots of the expected, worst and best case subsidy jump probability distribution functions are shown in Fig. 13 along with a reference case to better illustrate the positive skew and fat tail.

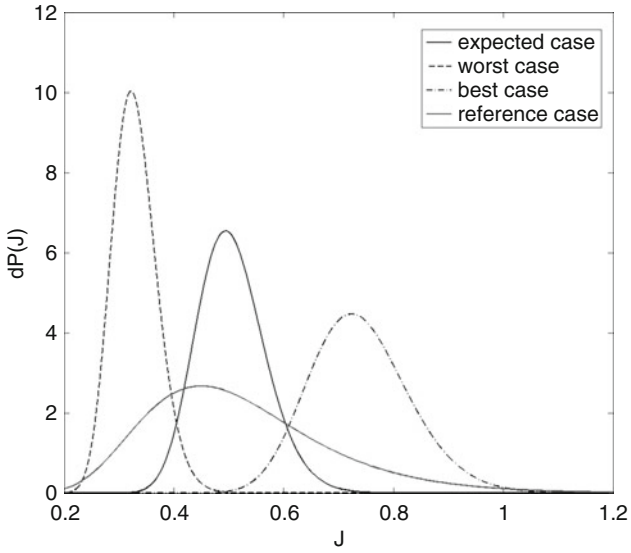

Fig. 13 The probability distribution functions $dP(J)$ of the jumps J of the expected case $LogN(-0.69, 0.015)$, worst case $LogN(-1.118, 0 : 015)$, best case $LogN(-0.309, 0.015)$, and a reference case $LogN(-0.7, 0.1)$ highlight the skew

To improve the model, more classes of jump distributions or non-constant Poisson arrival rates could be considered for future work. Another possible improvement to the expected subsidy jump model would be to incorporate management's views on the probability of possible policy outcomes or cases, each with an associated probability determined by management (an idea motivated by [20] but here simplified). This is both easier to justify to industry practitioners and greatly simplifies the analysis as it effectively removes the continuous variable J and replaces it with a discrete variable J_i. This reduces the dimensionality of the PID variational inequality system, which greatly reduces the computational time by reducing the problem to solving discrete weighted probabilities for each outcome J_i. For completeness, the integro operator would be replaced with $\mathscr{I}[V] = \lambda(\sum_i V_i P_i - V)$ and a PID variational inequality solved for each outcome i with associated value function V_i and management probability estimate P_i.

Appendix 1: Numerical Method

A brief exposition of the numerical method used to solve this PID variational inequality system is presented below. We refer the reader to [9, 14, 18, 28] for a more detailed analysis of the finite difference solutions to stochastic control problems and PIDEs.

The general PID variational inequality is of the form

$$\max\left[\frac{\partial V}{\partial t}+\mathscr{L}[V]+\mathscr{I}[V]+f-rV,\ \ h-V\right]=0. \tag{44}$$

where the differential operator is (occasionally suppressing any l, c, z dependence of μ, σ, a, b)

$$\mathscr{L}[V]=\mu\frac{\partial V}{\partial l}+a\frac{\partial V}{\partial c}+\frac{1}{2}\sigma^2\frac{\partial^2 V}{\partial l^2}+\rho\sigma b\frac{\partial^2 V}{\partial l\partial c}+\frac{1}{2}b^2\frac{\partial^2 V}{\partial c^2} \tag{45}$$

and the integro operator is

$$\mathscr{I}[V]=\lambda(E[V(l,c,J)]-V(l,c,z)) \tag{46}$$

and the constraint is

$$h=V_u-D_u \tag{47}$$

The numerical solution is obtained via finite differences at grid points $V(l_i,c_j,z_p,t_k)=V^k_{i,j,p}$ usually using second order centred differences except possibly at the boundary conditions. The grid points are

$$t_k=t_0+k\Delta t \tag{48}$$

$$l_i=l_0+i\Delta l \tag{49}$$

$$c_j=c_0+j\Delta c \tag{50}$$

$$z_p=z_0+p\Delta z \tag{51}$$

where the increments Δ need not necessarily be uniform. Divided differences are used to approximate the derivatives. Two are shown below for reference

$$\frac{\partial V}{\partial l}\approx\frac{V^k_{i+1,j,p}-V^k_{i-1,j,p}}{2\Delta l} \tag{52}$$

$$\frac{\partial V}{\partial t}\approx\frac{V^{k+1}_{i,j,p}-V^k_{i,j,p}}{\Delta t} \tag{53}$$

The integral $E[V(l,c,J)]$ is simply truncated and approximated along a grid as well

$$E[V(l,c,J)]\approx\int_0^{J_{max}}V(l,c,J)P(J)dJ\approx\sum_{p=0}^{P}V^k_{i,j,p}g(z_p)\Delta z \tag{54}$$

where the expectation is truncated by a point $J_{max} = z_P$ at which the error in the approximation is small. Note any kind of quadrature rule can be used along with non-uniform grid spacing besides the rule shown above.

A fitted scheme is used to write out a system of equations for $V^k_{i,j,p}$ at the grid points

$$\frac{V^{k+1} - V^k}{\Delta t} + \theta L V^{k+1} + (1-\theta) L V^k + \phi I V^{k+1} + (1-\phi) I V^k + f \leq 0 \tag{55}$$

where L is the differentiation matrix associated with the partial differential operator $\mathscr{L}$ including the source term $-rV$ and I is the integration matrix associated with the integro operator $\mathscr{I}$. The parameters θ and ϕ blend averages of the discretized PIDE at time steps k and $k+1$ (e.g. $\theta = 0$ is fully implicit and $\theta = \frac{1}{2}$ yields a Crank-Nicholson scheme). A small abuse of notation V^k refers to the entire collection of grid points i, j, p at time step k. The running profit function at all grid points is simply f. The differentiation matrix L tends to be stiff whereas the integration matrix I tends to be non-stiff allowing for the use of IMEX style time marching schemes.[4]

For reference, L can be considered a tensor that operates on a square $V_{i,j}$ at all p. In tensor notation, at the interior points L is for example

$$L_{i,j,i,j} = -\frac{2}{\Delta l^2}\frac{1}{2}\sigma^2_{i,j} - \frac{2}{\Delta c^2}\frac{1}{2}b^2_{i,j} - r \tag{56}$$

$$L_{i,j,i,j-1} = -\frac{1}{2\Delta c}a_{i,j} + \frac{1}{\Delta c^2}\frac{1}{2}b^2_{i,j} \tag{57}$$

$$L_{i,j,i-1,j-1} = \frac{1}{4\Delta l \Delta c}\rho\sigma_{i,j}b_{i,j} \tag{58}$$

where $L_{i,j,i+i^*,j+j^*} = 0$ if $|i^*|, |j^*| \geq 2$. Conditions must be applied along the boundary (e.g. linearity at far field). The integration matrix I is applied to a column $V_{i,j,p}$ across all p at a point (i, j), like a matrix in p constant across all i, j. For example,

$$I_{p,p} = \lambda\left[\frac{1}{2}g(z_p)(z_{p+1} - z_p) - 1\right] \tag{59}$$

$$I_{p,q} = \lambda\frac{1}{2}g(z_q)(z_{q+1} - z_{q-1}). \tag{60}$$

using a trapezoidal quadrature rule.

The system is solved subject to a known final condition $V(l, c, z, T) = Q(l, c, z)$ (being a backward Kolmogorov type equation). If there is no salvage value at the

[4]We note that using a Crank-Nicholson scheme in both L and I appeared to deliver good results.

end of the facility life $V^K_{i,j,p} = Q_{i,j,p} = 0$ (where $T = t_0 + K\Delta t$) but in general the salvage value should satisfy some inequalities around the switching costs D_{ij}.

This is a complementary problem

$$MV^k - b \leq 0, \quad h \leq V^k, \quad \left(MV^k - b\right)^T (V^k - h) = 0 \tag{61}$$

where superscript T denotes the matrix transpose. The matrix M is an aggregation of the integration and differentiation matrix pre-multipliers of V^k while b is a vector of collected knowns at time k (from $k + 1$). This matrix system is then solved using an iterative fixed point method similar to projected successive over-relaxation. Several iterative schemes for non-linear control problems are described in [1, 9, 10, 14, 18, 28, 37].

Appendix 2: Optimal Control

The intuition behind the proofs of the theorems in Sect. 3 are presented in this appendix.

Regarding the One-Dimensional Model Optimal Stochastic Control 3.1

Proof (Theorems 1 and 2). Consider the optimization with respect to λ

$$\inf_{\lambda_{min} \leq \lambda \leq \lambda_{max}} \mathscr{J}[V]. \tag{62}$$

Due to the boundedness of λ, this problem is nonsingular. Since $\mathscr{J}[V] = \lambda(E[V(y+J)] - V(y))$ is linear in λ, it achieves its critical values at the endpoints $[\lambda_{min}, \lambda_{max}]$ and the optimal λ satisfies

$$\lambda = \begin{cases} \lambda_{min} & \text{if } E[V(y+J)] - V(y) \geq 0, \\ \lambda_{max} & \text{if } E[V(y+J)] - V(y) < 0. \end{cases} \tag{63}$$

Turning now to the optimization with respect to α,

$$\inf_{\alpha_{min} \leq \alpha \leq \alpha_{max}} \lambda(E[V(y+J)] - V(y)) \Rightarrow \inf_{\alpha} E[V(y+J)] \tag{64}$$

where we drop the α bounds for notational brevity. The expectation can be written as

$$\inf_{\alpha} E[V(y+J)] = \inf_{\alpha} \int_{-\infty}^{\infty} V(y+J) g_N(J) dJ, \quad g_N \text{ is the normal kernel } N(\alpha, \beta^2) \tag{65}$$

$$= \int_{-\infty}^{\infty} \inf_{\alpha} \{V(y+\alpha+z)\} g_z^*(z) dz, \quad g_N^* \text{ is the kernel } N(0, \beta^2) \tag{66}$$

$$= \int_{-\infty}^{\infty} V(y+\alpha_{min}+z) g_z^*(z) dz \tag{67}$$

if $V(y)$ is monotone increasing in y which is true of the class of profit functions $f(y)$ considered in this analysis. (This result follows from the Feynman-Kac or Green's formula for $V(y)$ given $f(y)$ is monotone increasing.)

A similar argument applies for deriving the maximal optimal control (Theorem 2) but applied in the opposite direction.

Summarizing, the *worst case* project value is given by the minimal optimal control and the *best case* is given by the maximal optimal control subject to certain regularity conditions on V and f (namely monotonicity). □

Proof (Theorem 3). Note that the integro operator $\mathscr{I}$ is single-signed almost everywhere if f is such that $V(y)$ is convex and $\alpha = 0$. The justification follows from Jensen's inequality $V(E[y+J]) \leq E[V(y+J)]$ and that $E[y+J] = y+\alpha = y$. Thus

$$E[V(y+J)] - V(E[y+J]) = \tag{68}$$

$$E[V(y+J)] - V(y) = \frac{1}{\lambda} \mathscr{I}[V] \geq 0 \tag{69}$$

and accordingly $\lambda = \lambda_{min}$ for all y (and vice versa for the maximal control). □

Regarding the Constant Coefficient Option Price 3.1.1

Proof (Theorem 4). For a function $u(Y_t = y, t)$, applying Ito's lemma for jump diffusions results in

$$u(Y_T, T) - u(y, t) = \int_t^T b \frac{\partial u}{\partial y} dW_s + \int_t^T \left(\frac{\partial u}{\partial t} + a \frac{\partial u}{\partial y} + \frac{1}{2} b^2 \frac{\partial^2 u}{\partial y^2} \right) ds$$

$$+ \int_t^T [u(Y_s + J, s) - u(Y_s, s)] dN_t. \tag{70}$$

Taking the expectation causes the Ito integral to become zero (since $E[\int_t^T u dW_s|\mathscr{F}_t] = 0$ for smooth functions u). The expectation of the jump term becomes

$$E\left[\int_t^T [u(Y_s + J, s) - u(Y_s, s)]dN_t\right] = \int_t^T E_J\left[u(Y_s + J, s) - u(Y_s, s)\right]\lambda ds \tag{71}$$

since the Poisson arrivals dN_t and Brownian motion dW_t are independent, and $dN_t = 1$ with probability λds or 0 otherwise. Here E_J denotes an expectation with respect to J only (recall $J \perp W_t$).

When $u(\cdot, T) = 0$, and the jumps J and Brownian motion are independent, the expectation is

$$\begin{aligned} &E[u(Y_T, T) - u(y, t)] \\ &= -u(y, t) \\ &= E\left[\int_t^T \left(\frac{\partial u}{\partial t} + a\frac{\partial u}{\partial y} + \frac{1}{2}b^2\frac{\partial^2 u}{\partial y^2} + \lambda(E_J[u(Y_s + J, s)] - u(Y_s, s))\right) ds\right] \end{aligned} \tag{72}$$

If $u(y, t)$ satisfies the nonhomogeneous PIDE

$$\frac{\partial u}{\partial t} + a\frac{\partial u}{\partial y} + \frac{1}{2}b^2\frac{\partial^2 u}{\partial y^2} + \lambda(E_J[u(y + J, t)] - u(y, t)) = -f(y), \tag{73}$$

the solution has the probabilistic (Feynman-Kac) representation

$$u(y, t) = E\left[\int_t^T f(Y_s)ds \middle| Y_t = y\right] \tag{74}$$

The discounted value function $V(Y_s, s) = e^{-r(s-t)}u(Y_s, s)$ satisfies the PIDE of Theorem 4 and has probabilistic representation

$$V(y, t) = E\left[\int_t^T e^{-r(s-t)}f(Y_s)ds \middle| Y_t = y\right]. \tag{75}$$

The key to solving this expectation is to condition Y on n, the number of jumps so far, denoted $Y_{s,n}|n$. Note that the probability of observing n Poisson jumps over a time period $s - t$ is $P(n, s - t) = e^{-\lambda(s-t)}\frac{\lambda^n(s-t)^n}{n!}$. Thus

$$V = E\left(E\left[\int_t^T f(Y_{s,n})ds \middle| n\right]\right) \tag{76}$$

$$= \sum_{n=0}^{\infty}\int_{-\infty}^{\infty}\int_t^T e^{-\lambda(s-t)}\frac{\lambda^n(s-t)^n}{n!}e^{-r(s-t)}y_{s,n}^+ \frac{1}{\sqrt{2\pi B_{s,n}^2}}e^{-\frac{(y_{s,n}-A_{s,n})^2}{2B_{s,n}^2}} ds dy_{s,n} \tag{77}$$

where $A_{s,n} = y + a(s-t) + n\alpha$ and $B_{s,n}^2 = b^2(s-t) + n\beta^2$.

$$V = \sum_{n=0}^{\infty} \int_{-\infty}^{\infty} \int_{t}^{T} e^{-\lambda(s-t)} \frac{\lambda^n (s-t)^n}{n!} e^{-r(s-t)} (A_{s,n} + B_{s,n} z)^+ \frac{1}{\sqrt{2\pi}} e^{-\frac{z^2}{2}} ds dz \quad (78)$$

$$= \sum_{n=0}^{\infty} \int_{t}^{T} \int_{-d}^{\infty} e^{-\lambda(s-t)} \frac{\lambda^n (s-t)^n}{n!} e^{-r(s-t)} (A_{s,n} + B_{s,n} z) \frac{1}{\sqrt{2\pi}} e^{-\frac{z^2}{2}} dz ds \quad (79)$$

where $d = A_{s,n}/B_{s,n}$. Changing variables $x = -z$ and flipping the limits of integration yields

$$V = \sum_{n=0}^{\infty} \int_{t}^{T} e^{-\lambda(s-t)} \frac{\lambda^n (s-t)^n}{n!} e^{-r(s-t)} \times \left(\int_{-\infty}^{d} A_{s,n} \frac{1}{\sqrt{2\pi}} e^{-\frac{x^2}{2}} dx - \int_{-\infty}^{d} B_{s,n} x \frac{1}{\sqrt{2\pi}} e^{-\frac{x^2}{2}} dx \right) ds \quad (80)$$

$$V(y,t) = \sum_{n=0}^{\infty} \int_{t}^{T} e^{-\lambda(s-t)} \frac{\lambda^n (s-t)^n}{n!} e^{-r(s-t)} \left(A_{s,n} \Phi(d) + \frac{B_{s,n}}{\sqrt{2\pi}} e^{-\frac{d^2}{2}} \right) ds \quad (81)$$

where $\Phi(x)$ is the standard normal cumulative distribution function. □

Regarding the Complete Stochastic Control Problem 3.2

Proof (Theorems 5 and 6). The argument for obtaining the optimal λ is identical to the one-dimensional case. Determining the optimal α is similar to the previous case, but slightly more delicate. Again, it rests on the monotonicity of f. Recall

$$f_1(l,c,z) = \kappa(l + z - K_1) - c, \;\; f_0(l,c,z) = -\kappa K_0 \quad (82)$$

and thus f_1 is monotone increasing in z and f_0 is unaffected by z. By the Feynman-Kac representation for V_1 in Eq. 34, V_1 is monotone increasing in z. Similarly V_0, via the free boundary condition $V_0 = V_1 - D_{01}$ in Eq. 35, is monotone increasing in z by virtue of the boundary condition and regularity results along the free boundary [28, 29]. Now it remains to show that the expectation has a minimum

$$\inf_{\alpha} E[V(l,c,J)] = \inf_{\alpha} \int_{0}^{\infty} V(l,c,J) g_{LN}(J) dJ, \;\; g_{LN} \text{ is the lognormal kernel } LogN(\alpha, \beta^2) \quad (83)$$

$$= \int_0^\infty \inf_\alpha \{V(l, c, xe^\alpha)\} g^*_{LN}(x)dx, \ g_{LN} \text{ is the kernel } LogN(0, \beta^2) \tag{84}$$

$$= \int_0^\infty V(l, c, xe^{\alpha_{min}}) g^*_{LN}(x)dx \tag{85}$$

Summarizing, the PID variational inequality yields the *worst case* project value (minimal optimal control) when

$$\alpha = \alpha_{min}, \ \ \lambda = \begin{cases} \lambda_{min} & \text{if } E[V(l, c, J)] - V(l, c, z) \geq 0, \\ \lambda_{max} & \text{if } E[V(l, c, J)] - V(l, c, z) < 0 \end{cases} \tag{86}$$

and following a similar argument as above yields the *best case* value (maximal optimal control) when

$$\alpha = \alpha_{max}, \ \ \lambda = \begin{cases} \lambda_{max} & \text{if } E[V(l, c, J)] - V(l, c, z) \geq 0, \\ \lambda_{min} & \text{if } E[V(l, c, J)] - V(l, c, z) < 0 \end{cases} \tag{87}$$

□

References

1. Arnarson, T., Djehiche, B., Poghosyan, M., Shahgholian, H.: A PDE approach to regularity of solutions to finite horizon optimal switching problems. Nonlinear Anal. **79** (2009)
2. Avellaneda, M., Levy, A., Parás, A.: Pricing and hedging derivative securities in markets with uncertain volatilities. Appl. Math. Finance **27**, 73–88 (1995)
3. Baker, S.R., Bloom, N., Davis, S.J.: Measuring economic policy uncertainty. www.policyuncertainty.com (2013)
4. Bothast, R., Schlicher, M.: Biotechnological processes for conversion of corn into ethanol. Appl. Microbiol. Biotechnol.**67**, 19–25 (2005)
5. Brekke, K.A., Øksendal, B.: Optimal switching in an economic activity under uncertainty. SIAM J. Control. Optim. **32**, 1021–1036 (1994)
6. Brennan, M.J., Schwartz, E.S.: Evaluating natural resource projects. J. Bus. **58**, 135–157 (1985)
7. CBC: Ivanhoe 'surprised' by new Mongolian windfall tax. CBC News (2006). http://www.cbc.ca/news/business/ivanhoe-surprised-by-new-mongolian-windfall-tax-1.622422. Accessed 6 Jan 2014
8. CME: Chicago Mercantile Exchange commodity products: Trading the corn for ethanol crush
9. Cont, R., Voltchkova, E.: A finite difference scheme for option pricing in jump diffusion and exponential levy models. SIAM J. Numer. Anal. **3**(4), 1596–1626 (2005)
10. Cryer, C.W.: The solution of a quadratic programming problem using systematic overrelaxation. SIAM J. Control **9**, (1994)
11. Dixit, A.: Entry and exit decisions under uncertainty. Eur. J. Polit. Econ. **97**, 620–638 (1989)
12. Dixit, A., Pindyck, R.: Investment Under Uncertainty. Princeton University Press, Princeton (1994)

13. DOE: Department of Energy alternative fuels data center: laws and incentives "small ethanol producer tax credit" (2013). http://www.afdc.energy.gov/laws/law/US/352. Accessed 1 June 2013
14. Duffy, D.J.: Finite Difference Methdos in Financial Engineering: A Partial Differential Equation Approach. Wiley, West Sussex (2006)
15. EIA: US Energy Information Administration: Energy timelines ethanol (2012). http://www.eia.gov/kids/energy.cfm?page=tl_ethanol. Accessed 15 June 2012
16. Fisher, R.W.: Business decision-making "well nigh impossible" amid US policy uncertainty: Dallas fed chief. Financial Post (2012). http://opinion.financialpost.com/2013/06/04/u-s-economy-needs-clear-road-map/. Accessed 6 Jan 2014
17. Fleten, S.E., Haugom, E., Ullrich, C.J.: Keeping the lights on until the regulator makes up his mind! Midwest Finance Association 2012 Annual Meetings Paper (2012)
18. Forsyth, P.A., Vetzel, K.R.: Numerical methods for nonlinear PDEs in finance. In: Duan, J.C., Gentle, J., Hardle, W. (eds.) Handbook of Computational Finance, pp. 503–528. Springer, Berlin (2012)
19. Jaimungal, S.: Irreversible investments and ambiguity aversion. SSRN (2011). http://ssrn.com/abstract=1961786. Available at SSRN
20. Jaimungal, S., Lawryshyn, Y.: Incorporating managerial information into real option valuation (2011)
21. Kirby, N., Davison, M.: Using a spark-spread valuation to investigate the impact of corn-gasoline correlation on ethanol plant valuation. Energy Econ. **32**, 1221–1227 (2010)
22. Maenhout, P.J.: Robust portfolio rules and asset pricing. Rev. Financ. Stud. **17**, 951–983 (2004)
23. Maxwell, C., Davison, M.: Using real option analysis to quantify ethanol policy impact on the firm's entry into and optimal operation of corn ethanol facilities. Energy Econ. **42C**, 140–151 (2014)
24. McCarter, J.: Missauga Power Plant Cancellation Costs Special Report April 2013. Office of the Auditor General of Ontario (2013)
25. Merton, R.C.: Option pricing when underlying stock returns are discontinuous. J. Financ. Econ. **3**, 125–144 (1976)
26. NEO: Nebraska Energy Office: Nebraska energy statistics ethanol rack prices
27. NEO: Nebraska Energy Office: Ethanol production capacity by plant archive (2013). http://www.neo.ne.gov/statshtml/122_archive.htm. Accessed 1 June 2013
28. Øksendal, B., Sulem, A.: Applied Stochastic Control of Jump Diffusions. Springer, Berlin (2007)
29. Pham, H.: Continuous-Time Stochastic Control and Optimization with Financial Applications. Springer, Berlin (2009)
30. Reuters: Ontario drops plan for TransCanada power plant. Thomson Reuters (2010). http://www.reuters.com/article/2010/10/07/transcanada-ontario-idUSN0716951920101007. Accessed 6 Jan 2014
31. Reuters: Ontario looks set to cut green energy subsidies. Thomson Reuters (2011). http://uk.reuters.com/article/2011/11/02/canada-energy-renewable-idUKN1E7A10GV20111102. Accessed 6 Jan 2014
32. RFA: Renewable Fuels Association: Historic US fuel ethanol production (2014). http://www.ethanolrfa.org/pages/statistics. Accessed 15 Jan 2014
33. Samis, M., Davis, G., Laughton, D.: Using stochastic discounted cash flow and real option monte carlo simulation to analyse the impacts of contingent taxes on mining projects (2007)
34. Schmit, T., Luo, J., Tauer, L.: Ethanol plant investment using net present value and real options analyses. Biomass Bioenergy **33**, 1442–1451 (2009)
35. Shmuel, J.: Stop sitting on your cash piles, Carney tells corporate Canada. Financial Post (2012). http://business.financialpost.com/2012/08/22/dont-blame-the-loonie-for-weak-exports-carney-tells-caw/. Accessed 6 Jan 2014
36. USDA: US Department of Agriculture: Feed grains database
37. Wilmott, P., Dewynne, J., Howison, S.: Option Pricing: Mathematical Models and Computation. Oxford Financial Press, Oxford (1994)